Bio-Inspired Synthesis and Bio-activity of Ruthenium Nanoparticles from Tridax procumbens (Dagadi Pala) Leaf Extract

AJIT DEVALE
A.S.P. College (Autonomous) Devrukh Dist-Ratnagiri
SAMADHAN NIKALAJE
A.C.S. College, Lanja
NEERAJ R. PRASAD
School of Nanoscience and Technolgy, Shivaji University, Kolhapur
AMIT VARALE
dspmaspamitdr@gmail.com

A.S.P. College (Autonomous) Devrukh Dist-Ratnagiri

Research Article

Keywords: Synthesis, Bio-inspired Synthesis, Ruthenium nanoparticles, Tridax procumbens, nanotechnology.

Posted Date: April 24th, 2025

DOI: https://doi.org/10.21203/rs.3.rs-6160739/v1

Additional Declarations: No competing interests reported.

Version of Record: A version of this preprint was published at Discover Nano on September 7th, 2025.
See the published version at https://doi.org/10.1186/s11671-025-04300-z.

Abstract

Herein an attempt has been made to synthesize ruthenium nanoparticles (RuNPs) using Tridax procumbens leaf extract (Dagadi Pala) as a reducing and stabilizing agent. The synthesis was optimized by adjusting various parameters which includes temperature, concentration of leaf extract, and reaction time. The synthesized RuNPs was characterized using advanced characterization techniques such as UV-visible, XRD, EDAX, FTIR spectroscopy, SEM, TEM. The analysis indicates formation of nanoparticles with a uniform size and morphology. The biological properties of the as synthesized RuNPs were evaluated to determine their antimicrobial, antifungal, and antioxidant activities against various microbial strains. Results demonstrated significant antibacterial and antifungal properties alongside notable antioxidant activity, suggesting potential applications in biomedical fields. This study highlights the feasibility of utilizing Tridax procumbens leaf extract for environmentally friendly synthesis of ruthenium nanoparticles, opening opportunities for future research in nanotechnology and green chemistry.

1. Introduction

Green synthesis methods for nanoparticle production have emphasized significant attention due to environmentally friendly, profitable, and ecological nature [1][2]. Among various nanomaterials, ruthenium nanoparticles (RuNPs) have attracted interest in nanotechnology due to their distinct chemical properties, such as high catalytic activity, stability, and potential antimicrobial, antifungal, and antioxidant effects [3]. In contrast, conventional chemical and physical synthesis methods for RuNP production typically require toxic reagents and harsh conditions, which can harm human health and the environment [4–6].

Nanotechnology, which involves manipulating matter at the nanoscale, has paved the way for numerous innovations, especially in medicine, environmental science, and materials science. Among the diverse range of nanoparticles, metal nanoparticles have garnered considerable attention due to their exceptional physical, chemical, and biological characteristics. Ruthenium (Ru), a transition metal, has demonstrated significant potential in catalysis, drug delivery, and cancer treatment applications. Ruthenium nanoparticles (RuNPs) are particularly noteworthy for their potent bioactivity, which includes antibacterial [7–10], antifungal [11–13], and antioxidant effects [10, 14–15].

Using plant extracts as stabilizing and reducing agents has emerged as a promising alternative to address these challenges. Tridax procumbens, a well-known medicinal plant, contains bioactive compounds that may aid in the green synthesis of metal nanoparticles [16]. This report involved synthesizing ruthenium nanoparticles using *Tridax procumbens* leaf extract as both a reducing and stabilizing agent. The prepared nanoparticles were analysed through several techniques, including UV-visible, XRD, EDAX, FTIR spectroscopy, as well as SEM and TEM.

Along with their structural and morphological characterization, the biological activity of the RuNPs was evaluated to assess their potential for therapeutic applications. This study focuses on the ruthenium nanoparticles synthesized using leaf extract of *Tridax procumbens*, characterizing them, checking

stability, and assessing potential biological activities, including antibacterial, antifungal, and antioxidant properties [17–18]. The results are anticipated to enhance the existing knowledge in nanomedicine and environmental sustainability.

2. Methods

2.1 Plant material and extraction

Fresh leaves of *Tridax procumbens* were collected from the sub-campus in Devrukh, Sangameshwar, Ratnagiri, India. The leaves underwent a meticulous cleaning process involving repeated rinses with running water, culminating in a final rinse with double-distilled water. Subsequently, they were dried under shaded conditions at room temperature. After drying, the leaves were and grinded into fine powder with the help of a grinder. About 5.0-gram sample of dehydrated leaf powder was boiled in 100 mL of double-distilled water and maintaining a temperature of 50–60°C for 20 minutes. Using Whatman filter paper No. 1, the mixture was filtered. The subsequent filtrate was stored in a well-sealed bottle in the refrigerator at 5°C and was designated as the S1 extract.

2.2 Green synthesis of Ruthenium nanoparticles

The leaf extract of *Tridax procumbens* was mixed with 100 mL of a 2mmole of Ruthenium Choloride solution is heated between 60–70°C with constant stirring for about 60 minutes. Within 30 minutes, the reduction of Ru nanoparticles (RuNPs) became visibly evident. The initial brown colour slowly converted to a light blackish-yellow, indicates the formation of RuNPs (Fig. 1).

2.3 Characterization of RuNPs

The UV-Vis spectra of the synthesized nanoparticles were recorded using a Jasco Spectrophotometer V-770. X-ray diffraction pattern of the ruthenium nanoparticles was recorded on a BRUKER AXS D8 powder diffractometer by Cu Kα radiation (λ = 0.15425 nm), scanning from 20° to 80° (2θ). FTIR analysis was conducted with a JASCO FTIR-410 instrument (USA). To examine the chemical constituents, 1% KBr plates were prepared using the powdered samples and lyophilized plant extract.

A comprehensive analysis of the samples' surface morphology and elemental composition was conducted by SEM coupled with EDX on a JEOL JSM IT 200 tool. For interpretation of SEM, the dried leaf samples were gold-coated kept on carbon tape. The morphological characteristics of the prepared nanoparticles were analyzed by TEM using a Tecnai 120 G2 microscope with an operational voltage of 120 kV.

2.4 Biological Activities

Antimicrobial Assay:

The antimicrobial activities of the Ru nanoparticles were assessed against some Gram-negative bacterium such as E.coli [NCIM 2832] and P. aeruginosa [NCIM 9027] and Gram-positive bacterium like S. aureus [NCIM 5345] and B. cereus [NCIM 2703] to the test sample was assessed using the agar well diffusion assay [7–10]. Fresh bacterial cultures (24 hours old) were spread evenly on the surface of nutrient agar plates (Hi-Media) using a sterilized glass spreader to ensure uniform growth. Meanwhile, nanoparticle solutions were prepared by dissolving them in sterilized distilled water. Wells was formed on the nutrient agar plates using a sterilized stopper tool under aseptic conditions. Each well was then filled with 100 µL of the nanoparticle solution at 25 to 100 µg/mL concentrations. The plates were left in the refrigerator to allow proper diffusion of the nanoparticles within the agar. After incubating the plates at 37°C for 24 hours, they were visually examined to determine the presence and extent of antimicrobial activity. Streptomycin served as a positive control as well as sterile distilled water acted as a negative control.

Antifungal Assay:

Antifungal activities of Ru Nanoparticles were done by using the above procedure against *Aspergillus niger* [NCIM 1265] *and candida albicance* [NCIM 3471] fungal pathogens. Malt extract, Glucose, Yeast extract, and Peptone [MGYP] agar plates were used for this. Ketoconazole was used as the positive control, while sterile distilled water acted as the negative control [11–13].

Antioxidant assay:

The antioxidant properties of the synthesized nanoparticles were assessed by evaluating their capacity to neutralize the DPPH free radical using a scavenging activity assay. The reaction was carried out using 1 mL of the nanoparticle sample by varying concentrations of 2 mL of a 1.0 mmol/L solution DPPH radical in methanol ranging from 25µg to 100µg [10, 14–15]. The mixture was kept in the dark at 37°C for 30 minutes, after which the absorbance was determined at a wavelength of 570 nm using a Shimadzu UV-1800 spectrophotometer (Japan). The DPPH radical scavenging activity was measured using the following formula:

% Efficiency = [(Difference between Control and Sample Values) / Control Value] × 100.

The results are presented graphically, with ascorbic acid (concentration: 1000 µg/mL) as a reference standard (Graph 1).

3. Results and Discussion

3.1 Characterization of Nanoparticle

3.1.1 UV-Visible Spectroscopic Analysis of Nanoparticle

The formation of RuNPs was indicated through UV-visible spectroscopy. Measurements are verified over the wavelength range of 200–800 nm using a Jasco Spectrophotometer V-770, with a resolution set to 1 nm. The results, displayed in Fig. 2, show the formation of RuNPs, as indicated by an absorption peak at approximately 288 nm.

3.1.2 Infrared Spectroscopic Characterization using FT-IR

FTIR spectroscopy was used to identify several characteristic bands in the aqueous extract of *Tridax procumbens* which are associated with different functional groups. A peak at approximately 3438 cm^{-1}, characteristic of –OH stretching vibrations associated with water. Furthermore, the spectrum displayed peaks at 1397, 2925, 1460, 1524, and 1631 cm^{-1}, indicating the presence of aromatic compounds through C = C stretching of aromatic amines, aromatic C–H, asymmetric C = C–C stretching, symmetric –C–C = C stretching, and C = C stretching vibrations. The –C–H bending vibration was detected near 673 cm^{-1}, and a distinct peak at 539 cm^{-1} was attributed to metallic Ru. The C-H bending peak likely resulted from the reduction of $RuCl_3$ to RuNPs which is depicted in displayed in Fig. 3.

3.1.3 X-ray diffraction (XRD) analysis

The XRD pattern of the samples showed peaks at 20.68°, 30.00°, 41.51°, 46.84°, 58.43°, 66.97°, and 74.44°, corresponding to the (100), (002), (101), (102), (110), (220), and (311) planes, respectively, confirming the presence of RuNPs. The XRD patterns also exhibited characteristic peaks for RuO. These diffraction peaks are consistent with the features of spherical RuNPs.The results are shown in Fig. 4.

To determine the average particle size of the RuNPs, the Debye–Scherrer equation was used:

$$D= \frac{K\lambda}{\beta \cos\theta}$$

In this equation, the variables are defined as follows: D is the particle diameter in nanometers, K is the dimensionless Scherrer constant (approximately 0.94), λ denotes the X-ray wavelength, measured as 0.1541 nm; β represents the full width at half maximum (FWHM) of the diffraction peak, it is expressed in radians; and θ signifies the Bragg angle of diffraction. The calculated crystal sizes ranged from 10 to 20 nm, with an average size of 12.9 nm.

3.1.4 Morphological and Elemental Characterization using SEM and EDX

The morphological features and size distribution of the synthesized ruthenium nanoparticles was employed to investigate using SEM. Figures 5(a) and 5(b) display the scanning electron microscopy (SEM) images, revealing that the RuO nanoparticles predominantly exhibit a spherical morphology, with an average size of approximately 12.9 nm. Both magnifications of 10,000× (Fig. 5(a)) and 20,000× (Fig. 5(b)) highlight the narrow size distribution and the formation of spherical shapes.

The chemical composition of the RuNPs was characterized by EDX, and the corresponding results are presented in Fig. 6, which were produced using the leaf extract of *Tridax procumbens*. The EDX spectrum showed a peak at 2.6 keV, corresponding to ruthenium (Ru), along with smaller peaks associated with oxygen (O) and Sodium (Na). A peak observed at 2.6 kiloelectronvolts confirms the formation of metallic ruthenium through the reduction of ruthenium ions [19].

3.1.5 Characterization of Nanoparticles using TEM

The size distribution and shape of the synthesized ruthenium nanoparticles were characterized using TEM. As shown in the TEM image (Fig. 7), the synthesized Ru NPs displayed a relatively narrow size distribution, with an average diameter of 11.30 nm and individual particle sizes ranging from 2.00 nm to 22 nm. TEM analysis reveals that the synthesized Ru NPs generally have a spherical shape.

3.2 Biological Activity Analysis

3.2.1 Antimicrobial Activity

The antimicrobial properties of the ruthenium nanoparticles synthesized in this study were assessed using a modified agar healthy diffusion technique. The zones of inhibition against various bacterial pathogens are summarized in Table 1. The antimicrobial activity of the Ru nanoparticles was tested at concentrations varying from 25 to 100 µg/mL. No antimicrobial activity was observed at a concentration of 25 µg/mL. However, at 50 µg/mL and above concentrations, a distinct inhibition zone was observed against both Gram-positive and Gram-negative bacteria. This study concludes that the synthesized nanoparticles exhibit significant antimicrobial properties of the sample were assessed against a selection of clinically relevant bacterial pathogens, comprising B. cereus, S. aureus, E. coli, and P. aeruginosa. These findings suggest that these nanocomposites could effectively combat future bacterial infections. The results are tabulated in Fig. 8.

Table 1
Antimicrobial activity of Ru NPs against different test pathogens

Tested pathogens	**Zone of inhibition in millimetres (mm)**					
	1 (25µg/mL)	2 50µg/mL	3 75µg/mL	4 100 µg/mL	Streptomycin	Water
B. Cereus	00	24	26	29	30	00
S. aureus	00	22	24	27	29	00
P. aeruginosa	00	21	25	29	31	00
E. coli	00	20	21	00	27	00

3.2.2 Antifungal activity:

As per this study, Ru nanoparticles didn't show any antifungal activity [No zone of inhibition] against *Aspergillus niger*, but they showed antifungal activity from 75 µg/ml to 100 µg/ml against *candida alliance*: The results are tabulated in Fig. 9, Table 2.

Table 2
Antifungal Activity of Ru NPs against different test fungus

Tested pathogens	**Zone of inhibition in millimetres (mm)**					
	1	2	3	4	Ketoconazole	Water
Aspergillus niger	00	00	00	00	28	00
candida albicance	00	00	24	26	29	00

3.2.3 Antioxidant activity

The studied nanoparticle shows excellent scavenging activity, with the highest activity observed at 77.13 ± 0.64% scavenging activity at 100 µl concentration, followed by 75 µl (59.34 ± 1.12%), 50 µl (58.24 ± 1.58%), and 25 µl (51.47 ± 0.21%) of nanoparticle concentration. The results are shown in Fig. 10,

4. Conclusion

This research presents an environmentally friendly approach for synthesizing Ru nanoparticles (NPs) using leaf extract from *Tridax procumbens*. X-ray diffraction (XRD) analysis indicated that the Ru NPs exhibited high crystallinity, with an average crystalline size of 12.7 nm. Transmission electron microscopy (TEM) images revealed that the particles were spherical, with an average diameter of 11.3 nm. UV-visible spectroscopy, spanning the range of 200–800 nm, confirmed the successful formation of Ru NPs. The antibacterial properties of the Ru NPs were more prominent against Gram-positive bacteria than Gram-negative bacteria. Moreover, the synthesized Ru NPs showed antifungal activity against *Candida albicans*. The nanoparticles were non-toxic to bacteria and exhibited enhanced antioxidant activity. This green synthesis method is rapid, simple, cost-effective, time-efficient, and environmentally safe. This technique can be extended to synthesizing metal and metal oxide nanoparticles.

Declarations

Acknowledgements The authors appreciate the support and facilities provided by their respective institutions, which facilitated the completion of this work.

Author contributions Neeraj Prasad and Ajit Devale conceived and designed the experiments; Ajit Devale performed the experiments; Ajit Devale and Amit Varale analysed the data; Samadhan Nikalaje prepared the draft; and Amit Varale supervised for the present investigation. All authors reviewed and approved the final manuscript.

Funding This research did not receive any specific grant from funding agencies in the public, commercial, or not-for-profit sectors.

Data availability “Data is provided within the manuscript”.

Ethical approval Not applicable

Consent for publication All authors are aware of this submission.

Competing interests The authors declare no competing interests.

If your study is a clinical trial – Not Applicable

Consent to Participate declaration: Not applicable

References

1. Prasad R, Williams L, etc al. Applications of photogenic ZnO nanoparticles: A review on recent advancements. Journals of molecular liquid. 2021; 331(6):115805.
2. Vijayaram S, etc al. Applications of Green Synthesized Metal Nanoparticles — A Review. Biological Trace Element Research. 2024;202: 360–386.
3. Gupta PK, Mishra L. Ecofriendly ruthenium-containing nanomaterials: synthesis, characterization, electrochemistry. Bioactivity and catalysis Nanoscale Adv. 2020;5(2):1774–1791
4. Khan Z, Hussain JI, Hashmi AA. Shape-directing role of cetyltrimethylammonium bromide in the green synthesis of Ag-nanoparticles using Neem (Azadirachta indica) leaf extract, Colloids and Surfaces B: Biointerfaces. 2012;95: 229–234.
5. Song JY, Jang HK, Kim BS. Biological synthesis of gold nanoparticles using Magnolia kobus and Diopyros kaki leaf extracts. Process Biochemistry.2009;44:1133–1138.
6. Khalil MH, Ismail EH, etc al. Biosynthesis of Au nanoparticles using olive leaf extract. Arabian Journal of Chemistry.2012;5: 413–437.
7. Rautela A, Rani J, Debnath M. Green synthesis of silver nanoparticles from Tectona grandis seeds extract: characterization and mechanism of antimicrobial action on different microorganisms. Journal of Analytical Science and Technology. 2009;10(5).
8. Singh R, Hano C, Nath G, Sharma B. Green Biosynthesis of Silver Nanoparticles Using Leaf Extract of Carissa carandas L. and Their Antioxidant and Antimicrobial Activity against Human Pathogenic Bacteria. Biomolecules. 2021;11(2): 299.
9. Otari SV, Patil RM, etc al. Green biosynthesis of silver nanoparticles from an actinobacteria Rhodococcus sp. Materials Letters. 2012; 72:92–94.
10. Ubale P, Mokale S, etc al. Evaluation of in vitro anticancer, antimicrobial and antioxidant activities of new Cu (II) complexes derived from 4 (3H)-quinazolinone: Synthesis, crystal structure and molecular docking studies. Journal of Molecular Structure. 2022;1251: 131984.

11. Rangayasami A, etc al. Bioengineered silver nanoparticles using Elytraria acaulis (L.F.) Lindau leaf extract and its biological applications. Biocatal. Agric. Biotech. 2020; 27:101690.
12. Priya M, Venkatesan R, Deepa S. Green synthesis, characterization, antibacterial, and antifungal activity of copper oxide nanoparticles derived from Morinda citrifolia leaf extract. Scientific reports. 2023; 13:18838.
13. Mali SC, Dhaka A, Githala CK, Trivedi R. Green synthesis of copper nanoparticles using Celastrus paniculatus Willd. Leaf extract and their photocatalytic and antifungal properties. Biotechnology Reports. 2020; 27: e00518.
14. Ansari MI, Khan SA. Synthesis and antimicrobial activity of some novel quinoline-pyrazoline-based coumarinyl thiazole derivatives. Medicinal Chemistry Research.2017;26:1481–1496.
15. Gurav R, etc al. Rust-derived Fe_2O_3 nanoparticles as a green catalyst for the one-pot synthesis of hydrazine thiazole derivatives. Organic & Biomolecular Chemistry.2020;*18*(24):4575–4582.
16. Kumar K, Sheba A. A Study on Phytochemicals, Antimicrobial, And Synergistic Antimicrobial Activities of Hibiscus Sabdariffa, Asian Journal of Pharmaceutical and Clinical Research.2019;12(4):198–201.
17. Kannan SK, Sundrarajan M. Green synthesis of ruthenium oxide nanoparticles: Characterization and its antibacterial activity. Advanced Powder Technology. 2015;26(6):1505–1511.
18. Manjare SB, etc al. Biosynthesis of silver nanoparticles using leaf and bark extract of Indian plant carissa calendars, characterization and antimicrobial activity. Asian Journal of Nanoscience and Materials. 2020;2(1):58–66.
19. Gupta S, Giordano C, Gradzielski M, Mehta SK. Microwave-assisted synthesis of small Ru nanoparticles and their role in the degradation of congo red. J. Colloid Interface Sci. 2013;411:173–181.

Figures

Figure 1

Synthesis of Ru NPs

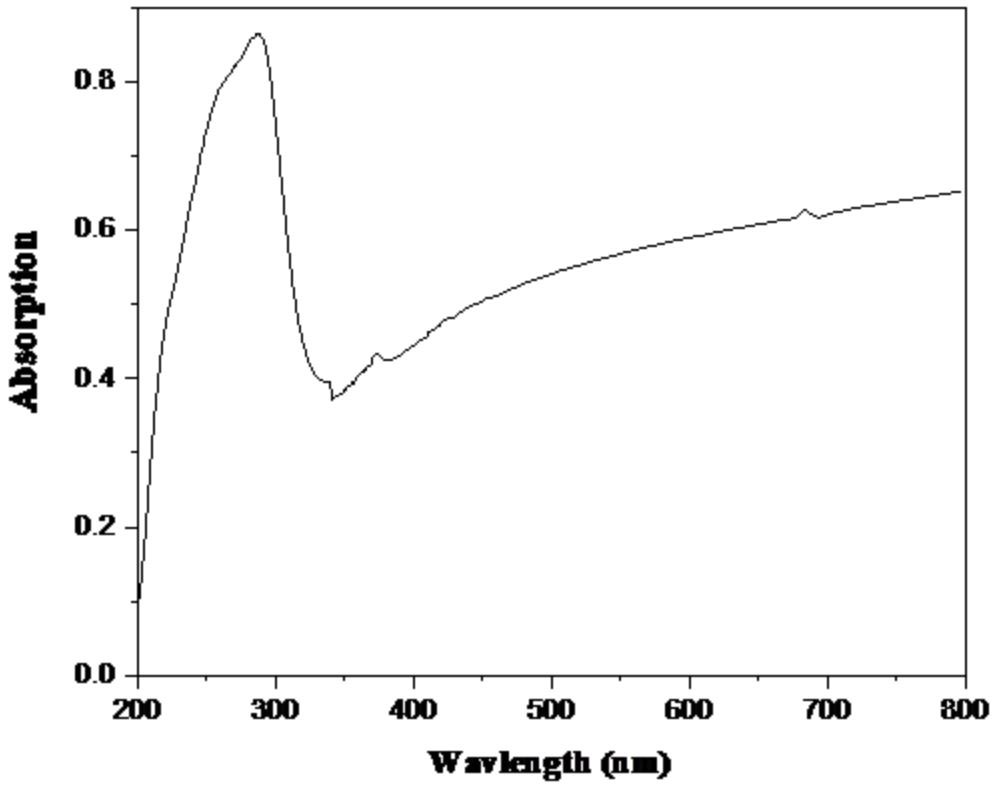

Figure 2

UV–Vis spectrum of synthesized RuNPs

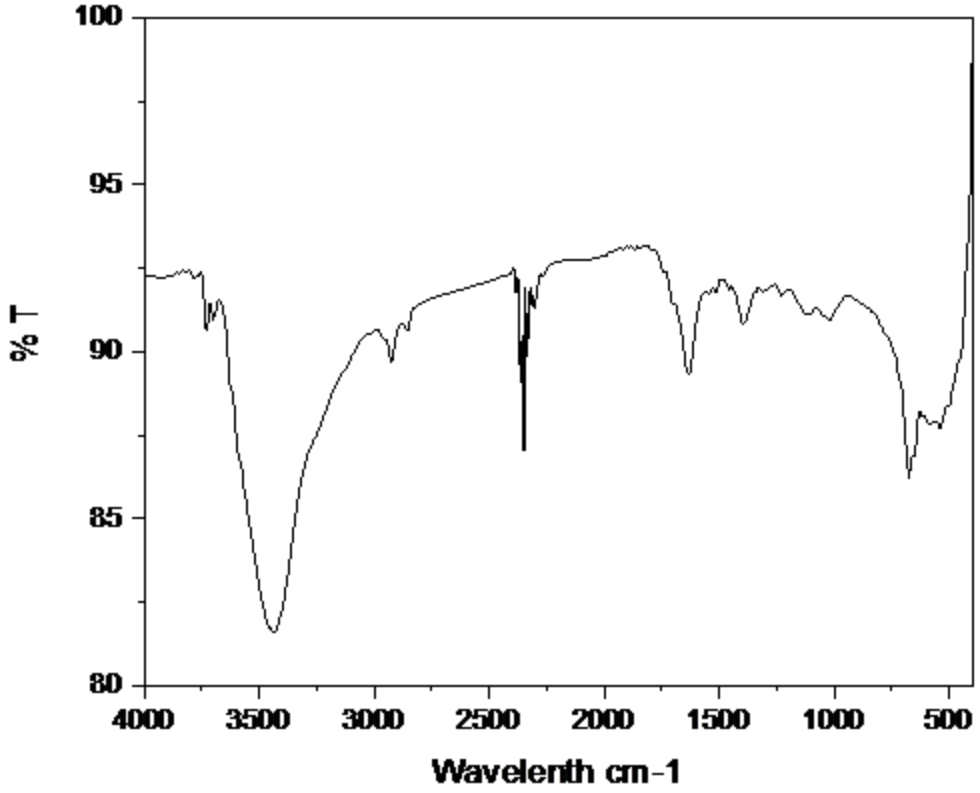

Figure 3

FT-IR spectra of synthesized RuNPs

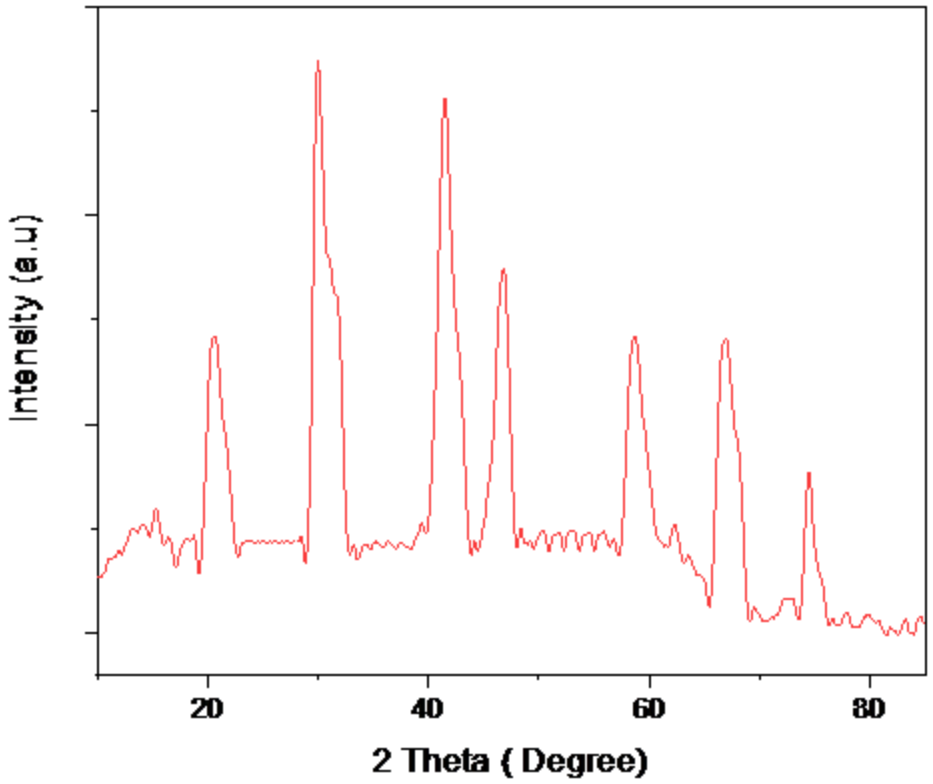

Figure 4

X-ray diffraction pattern of the synthesized Ru nanoparticles.

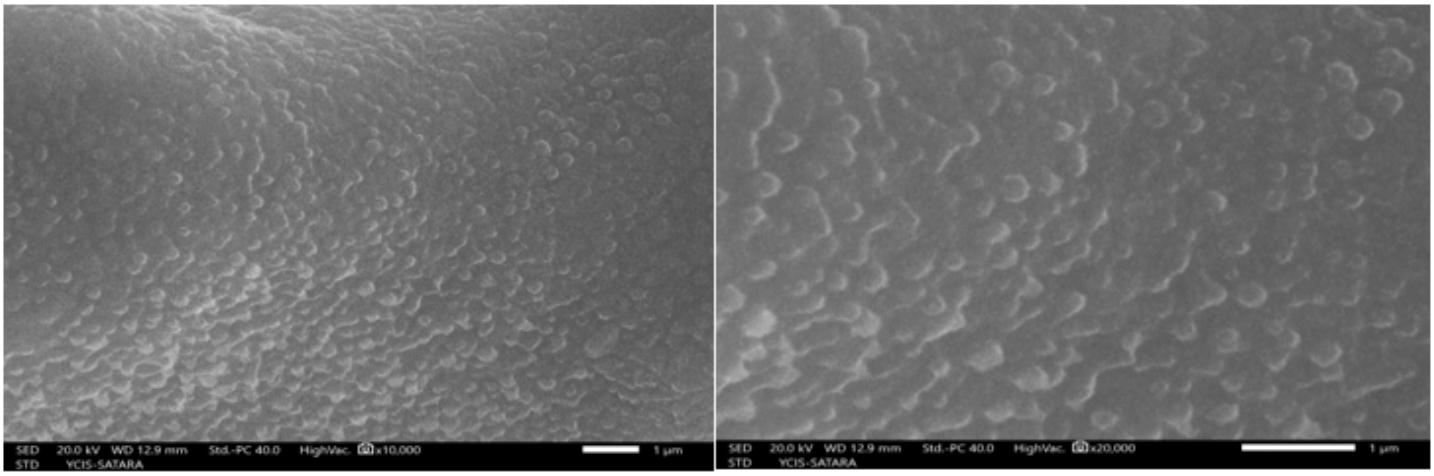

Figure 5

(a) and 5(b) SEM images show the synthesized RuNPs' morphology.

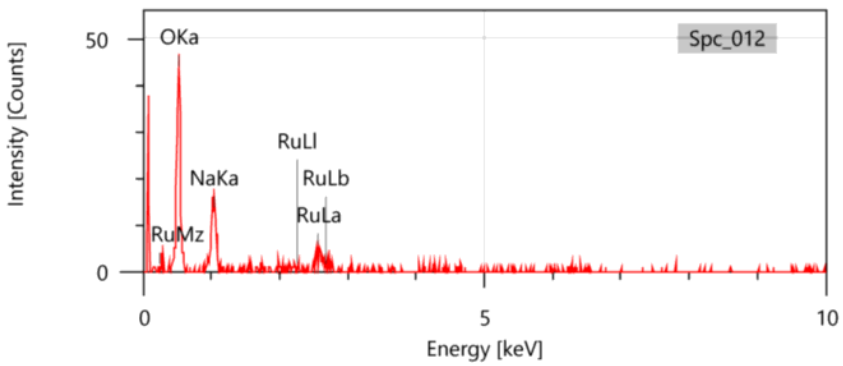

Display name	Standard data	Quantification method	Result Type
Spc_012	Standardless	ZAF	Metal

Element	Line	Mass%	Atom%
O	K	65.39±4.20	78.51±5.04
Na	K	23.10±3.03	19.30±2.53
Ru	L	11.51±2.40	2.19±0.46
Total		100.00	100.00
Spc_012			Fitting ratio 0.5959

Figure 6

The energy-dispersive X-ray spectroscopy (EDX) of the synthesized Ru nanoparticles

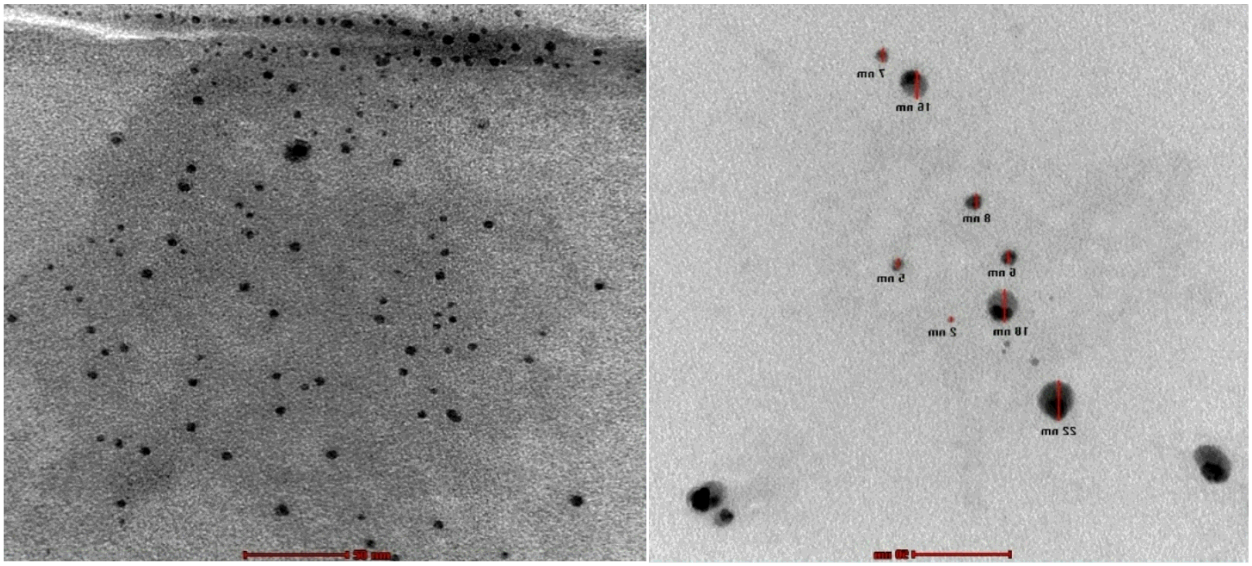

Figure 7

TEM analysis of Synthesized Ru NPs

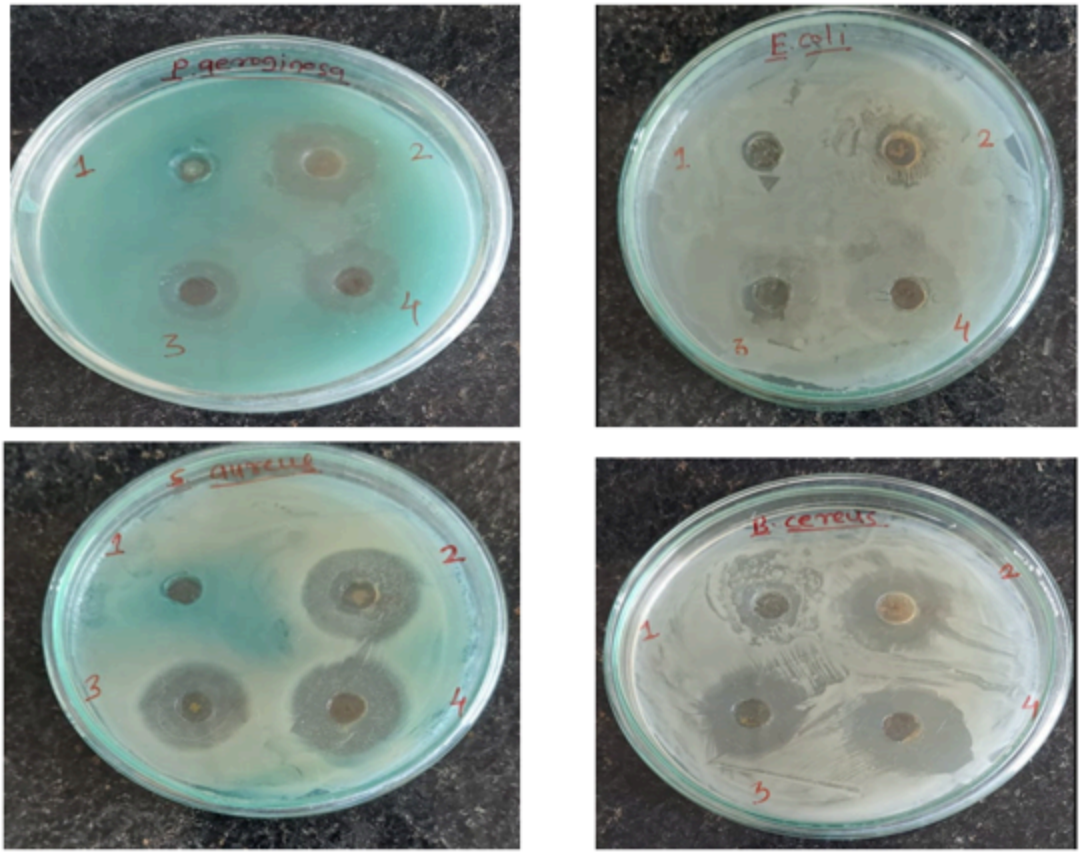

Figure 8

Antimicrobial activity of Ru NPs against different test pathogens

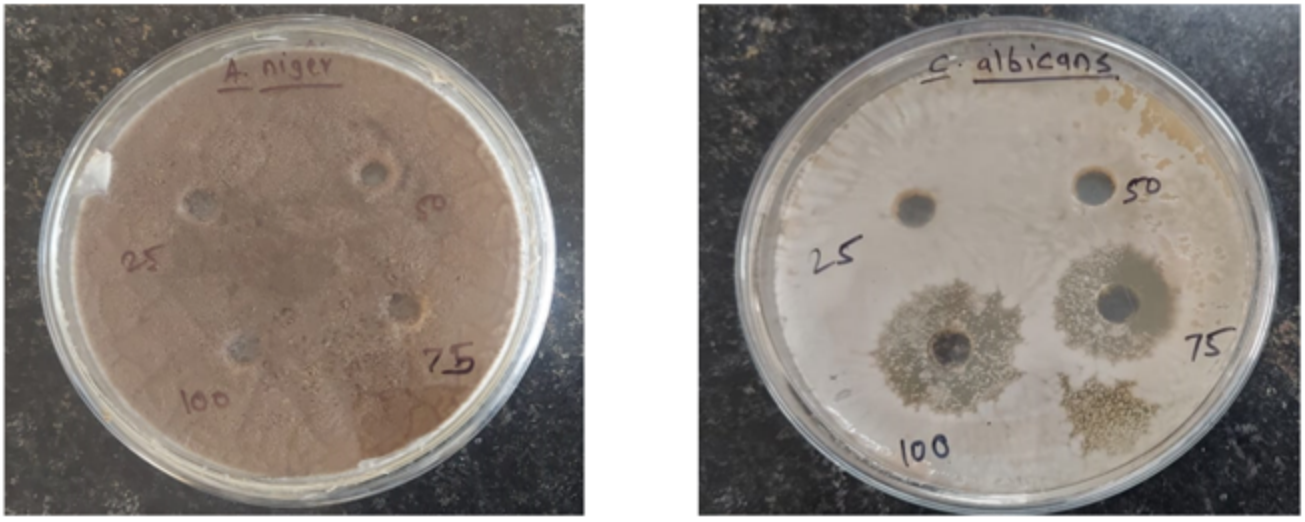

Figure 9

Antifungal Activity of Ru NPs against different test fungus

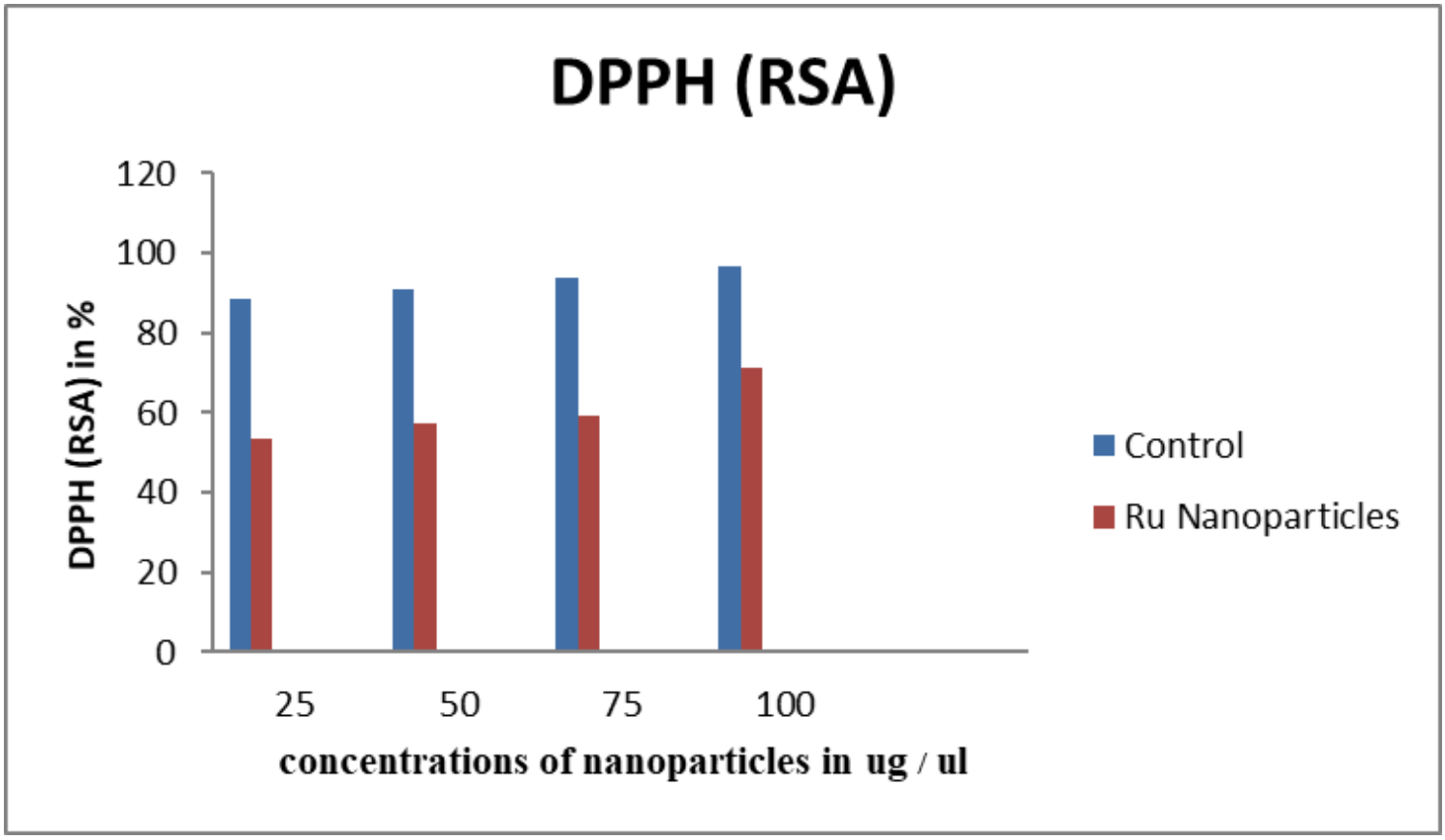

Figure 10

Antioxidant activity of nanoparticles

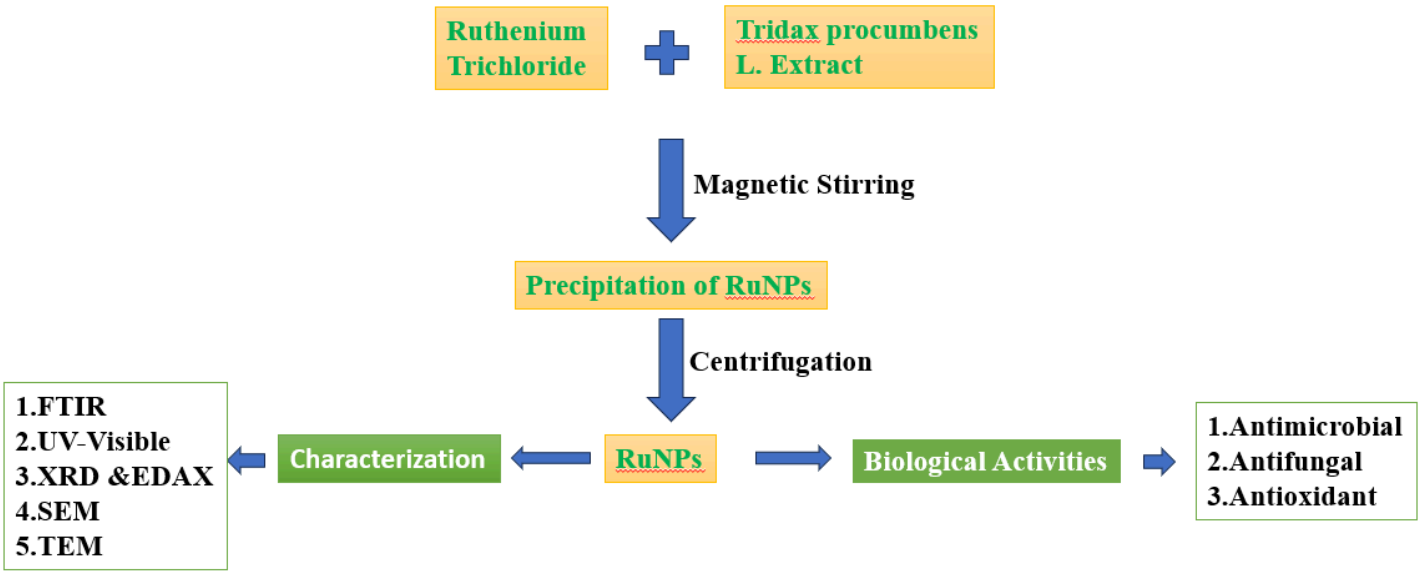

Figure 11

Unnumbered image in the Introduction section.

Schematic Illustration of the Synthesis, Characterization, and Biological Applications of Copper Ruthenium Nanoparticles.